

## Laser interaction with low-density carbon foam

S CHAURASIA<sup>1,\*</sup>, S TRIPATHI<sup>1</sup>, D S MUNDA<sup>1</sup>, G MISHRA<sup>1</sup>, C G MURALI<sup>1</sup>,  
N K GUPTA<sup>1</sup>, L J DHARESHWAR<sup>1</sup>, A K ROSSALL<sup>2</sup>, G J TALLENTS<sup>2</sup>,  
RASHMI SINGH<sup>3</sup>, D K KOHLI<sup>3</sup> and R K KHARDEKAR<sup>3</sup>

<sup>1</sup>Laser & Neutron Physics Section, Bhabha Atomic Research Centre,  
Mumbai 400 085, India

<sup>2</sup>Department of Physics, University of York, York, YO105 DD, UK

<sup>3</sup>Target Lab, Raja Ramanna Centre for Advanced Technology, Indore 452 013, India

\*Corresponding author. E-mail: pgshivanand@gmail.com

**Abstract.** Experiments were performed with a 15 J/500 ps Nd:glass laser ( $\lambda = 1064$  nm) focussed to an intensity  $>10^{14}$  W/cm<sup>2</sup>. X-ray emissions from carbon foam and 5% Pt-doped carbon foam of density 150–300 mg/cc were compared with that of the solid carbon targets. The thickness of the carbon foam was 15  $\mu$ m on a graphite substrate. X-ray emission was measured using semiconductor X-ray diodes covered with various filters having transmissions in different X-ray spectral ranges. It covered X-ray spectrum of 0.8–8.5 keV range. The X-ray emission in the soft X-ray region was observed to increase to about 1.8 times and 2.3 times in carbon foam and Pt-doped foam, respectively with respect to solid carbon. In hard X-rays, there was no measurable difference amongst the carbon foam, Pt-doped carbon foam and solid carbon. Scanning electron microscope (SEM) analysis demonstrates that foam targets smoothens the crater formed by the laser irradiation.

**Keywords.** Low-density foam; X-ray emission; volume absorption.

**PACS Nos** 52.50.Jm; 52.38.Ph; 52.38.Mf

### 1. Introduction

The use of low-density porous media as components of various types of the targets illuminated by high-power laser pulses is a very promising approach to study the physics of interaction between a laser beam and matter, and can lead to the successful resolution of a number of important scientific and technical problems. The interaction of laser light with the low-density porous or foam-like material is considered as very important and suitable in advanced inertial confinement fusion (ICF) target design. In the direct drive scheme, it is possible to significantly alter the spatial density distribution of the plasma corona that forms at the illuminated surface of a spherical thermonuclear target by depositing, on the surface, a layer of foam material with a suitably chosen thickness and initial density made from elements with low atomic numbers [1–3]. This will lead to efficient smoothing, i.e.

uniform energy deposition, to the targets in direct drive ICF. In the indirect drive scheme, implosion efficiency of the fuel pellet directly depends on the laser to X-ray conversion efficiency of the hohlraum walls. Research is still on to find methods for improving the amount of X-rays that reach the capsule [4]. Extreme ultraviolet (EUV) lithography is considered as an attractive method to succeed conventional optical lithography in the coming years. By using solid Sn targets, the spectrum is observed to be very broad around 13 nm which is not desirable. Sn doped in hydrocarbon foam can be used to control the spectral emissions from tin-doped targets for extreme ultraviolet lithography [5].

Experiments presented in this paper show an enhanced X-ray emission from pure carbon foams and platinum-doped carbon foams compared to that from solid carbon targets.

## 2. Experiments

The experiments were performed with our home-built Nd:glass laser system ( $\lambda = 1.064 \mu\text{m}$ ) which is capable of producing 16 J energy per pulse [6]. The laser system used consisted of a commercial oscillator (100 mJ/300–800 ps), five linear amplifiers of increasing diameter, two Faraday isolators and two spatial filter units. The high-power laser was focussed with an  $f/5$  lens into a chamber evacuated to  $4 \times 10^{-5}$  mbar providing intensities of the order of  $10^{13}$ – $2 \times 10^{14}$  W/cm<sup>2</sup>. Laser was incident normal to the target. Four silicon semiconductor diodes (XUV100, by UDT sensor) were used for X-ray flux measurement. The diodes were covered with different X-ray transmission filters to cover broad spectral range. The filters used were 5  $\mu\text{m}$  Al (transmission 0.8–1.56 keV), B10 (transmission >0.9 keV), 20  $\mu\text{m}$  Al (transmission >3.4 keV) and 5  $\mu\text{m}$  nickel (transmission 5–8.32 keV). Planar foil targets were used instead of hohlraum cavities, for the ease of fabrication and measurements. The laser focal spot size being of the order of 100  $\mu\text{m}$ , which is small compared to the diameter of hohlraum cavities that are generally used (a few mm), a planar foil can be assumed to simulate a part of the cavity wall. Two types of targets, foils of pure and platinum-doped carbon foams, were used in the experiments. Carbon foam was prepared by dissolving resorcinol and furfuraldehyde in isopropyl alcohol (IPA). Nonionic surfactant was added to the solution and after about 10 min stirring, potassium hydroxide was added as a base catalyst for initial particle formation, and the solution was maintained at 60°C for 2 h in an oven. For the platinum-doped foam sample, a metal precursor solution was obtained by dissolving hydrogen hexachloroplatinate in IPA which was then added to the initial solution. For undoped samples, hydrochloric acid was used as acid catalyst for gelation. Resorcinol furfural solution turned transparent green and immediately black on acidification. The solution was kept in a sealed vial and kept at 60°C for 65 h. Gel was formed by polycondensation of resorcinol with furfuraldehyde within 30 min. Additional 65 h curing was done for complete gelation and gel strengthening. The aged alcogels were removed from the oven and kept open for drying in air at ambient temperature. Dried bulk was ground in a ball mill and uniform distribution of particles less than 10  $\mu\text{m}$  was obtained. The powder was mixed with PVDF solution. The ratio of powder to PVDF (polyvinylidene fluoride)

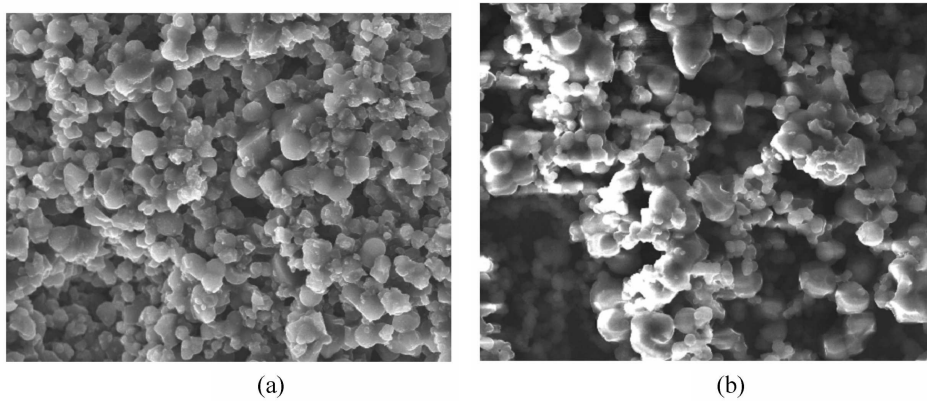


**Figure 1.** (a) SEM record of carbon foam and (b) Pt-doped carbon foam.

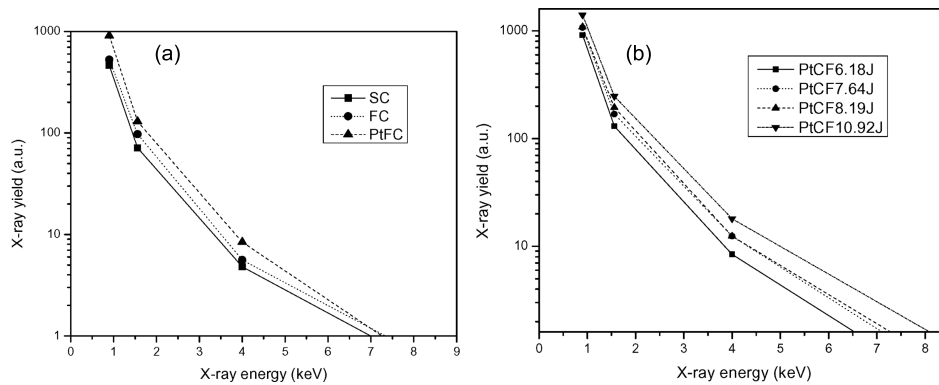


**Figure 2.** (a) X-ray spectrum recorded with various diodes covered with different X-ray filters for solid carbon (■), carbon foam (●) and Pt-doped carbon foam (▲). (b) X-ray spectrum of Pt-doped carbon foam for various laser energies.

was 4:1. This paste was then applied to a graphite sheet substrate to make thin films and then it was dried in oven at 15°C. The crater analysis was done using SEM images. The platinum-doped and undoped foam targets are shown in figures 1a and b.

### 3. Result and discussion

X-ray flux from pure and platinum-doped carbon foams was measured in the spectral range 0.7–8.3 keV by the X-ray detectors covered with different X-ray transmission filters. The X-ray transmission in the spectral range 0.7–8.5 keV is measured using various X-ray transmission filters. The X-ray emission from the solid carbon, carbon foam and Pt-doped carbon foam at a laser energy of 8 J is plotted in

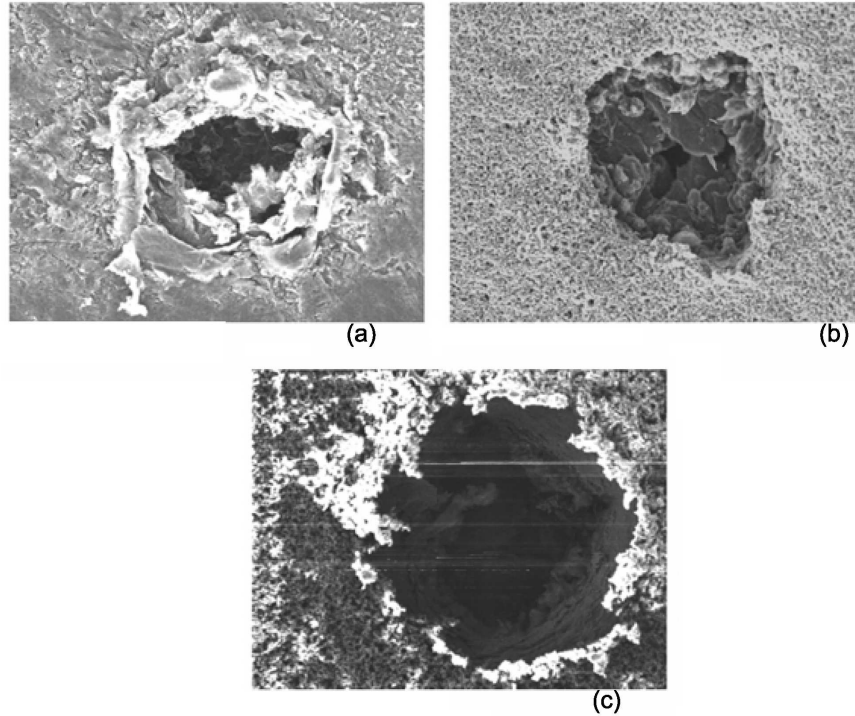


**Figure 3.** SEM records of the crater at laser energy 8 J/500 ps in (a) solid carbon, (b) carbon foam and (c) Pt-doped carbon foam.

figure 2. It is clear from figure 2a that the soft X-ray (0.7–1.56 keV) emission from the foam is about 1.8 times compared to that with the solid carbon. By adding 5% of Pt in the carbon foam, soft X-ray emission increases by a factor of 2.3 compared with the solid carbon. But, there is no appreciable difference (1.05 and 1.1 times as compared to 1.8 and 2.3 for soft rays) among the three for hard X-ray (5–8.32 keV) as seen in figure 2a. The X-ray spectrum for various laser energies for the Pt-doped foam is shown in figure 2b. It is observed from figure 2b, that the X-ray emission in the whole spectral range increases with the laser energy (intensity). Figure 3 shows the crater formations in the solid carbon, carbon foam and Pt-doped carbon foam. It is clearly observed that for the same laser energy and the same focal spot, the crater formation in the case of foam is smoothened. The size of crater increased for Pt-doped carbon foam which may be due to the increased lateral heat transport because of the presence of Pt. Analysis of the signals from the X-ray diode and comparison with a model of free-free and free-bound emission given in [7] allows for temperature determination of the plasma. This analysis when carried out for our spectrum shows that the plasma produced in our experiments has a two-temperature bi-Maxwellian distribution where the second temperature is a small fraction ( $F = 0.1\%$ ) of suprathermal electrons. It is indicated (figure 4) that the carbon foam target produces plasma with a thermal temperature

*Laser interaction with low-density carbon foam*

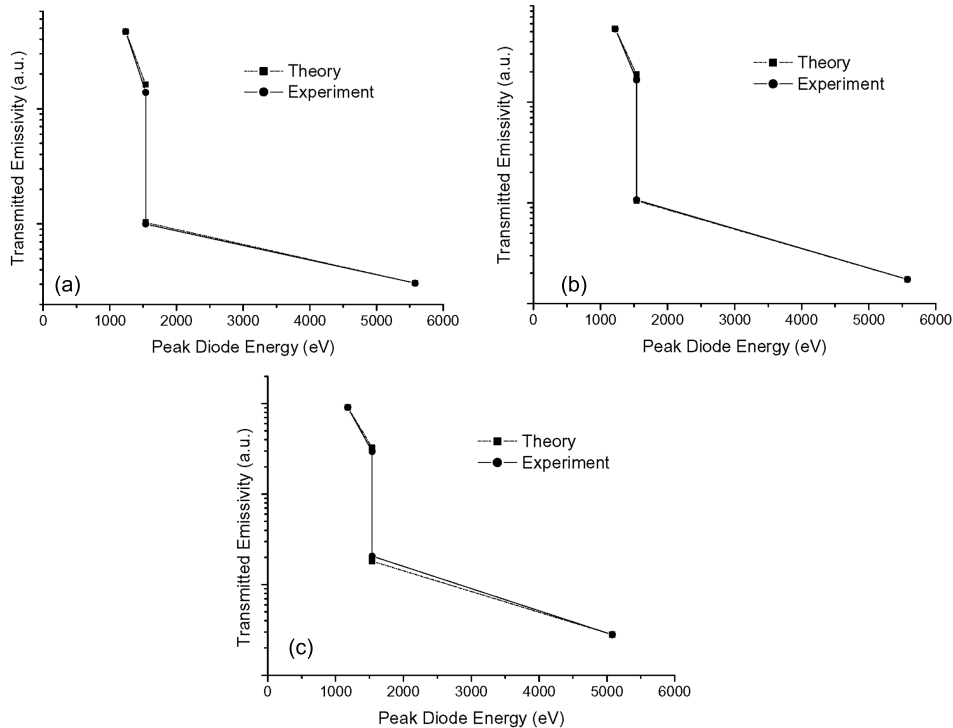


**Figure 4.** Transmitted emissivity as a function of peak transmitted energy for diode array and comparison with free-free and free-bound emissivity models [7] to determine temperature at similar laser energies. Plots representing (a) solid carbon, (b) carbon foam and (c) Pt-doped carbon foam have been normalized to the low energy channel. Temperatures determined are: Solid carbon –  $T_c = 230$  eV,  $T_h = 3.5$  keV, carbon foam –  $T_c = 240$  eV,  $T_h = 3.5$  keV and Pt-doped carbon foam –  $T_c = 250$  eV,  $T_h = 2.5$  keV.

10 eV higher than that of the solid target (230 eV), which accounts for the increase in soft X-ray emission. The Pt-doped target demonstrates a further increased thermal temperature of 250 eV as compared to a temperature of 230 eV calculated for solid carbon and a decrease in the suprathreshold temperature to 2.5 keV from 3.5 keV produced by the other targets. This increase in the thermal temperature and the decrease of the suprathreshold temperature for Pt-doped carbon foam explain the observed spectrum in this case.

**References**

- [1] S E Bodner, D G Colombant, A J Schmitt and M Klapisch, *Phys. Plasmas* **7**, 2298 (2000)
- [2] D G Colombant, S E Bodner, A J Schmitt, M Klapisch, J H Gardner, Y Aglitskiy, A V Deniz, S P Obenschain, C J Pawley and V Serlin and J L Weaver, *Phys. Plasmas* **7**, 2046 (2000)

- [3] M Dunne, M Borghesi, A Iwase, M W Jones, R Taylor, O Willi, R Gibson, S R Goldman, J Mack and R G Watt, *Phys. Rev. Lett.* **75**, 3858 (1995)
- [4] M D Rosen and J H Hammer, *Phys. Rev.* **E72**, 056403 (2005)
- [5] S S Harilal, B O'Shay, M S Tillack, Y Tao, R Paguio, A Nikroo and C A Back, *J. Phys. D: Appl. Phys.* **39**, 484 (2006)
- [6] S Chaurasia, C G Murali, D S Munda, N K Gupta, L J Dhareshwar, R Vijayan and B S Narayan, BARC Report BARC/2008/E/006 (2008)
- [7] I H Hutchinson, *Principles of plasma diagnostics*, 2nd ed. (Cambridge University Press, Cambridge, 2002) p. 200